Smart Agricultural Technology 9 (2024) 100642

Contents lists available at ScienceDirect

Smart Agricultural Technology

journal homepage: www.journals.elsevier.com/smart-agricultural-technology

Integrating solar induced fluorescence with high throughput plant screening for advanced phenotyping of plants

Amir Mayo [a], Snir Vitrack-Tamam [b], Menachem Moshelion [a], Oded Liran [b,1,*]

[a] Robert H. Smith Faculty of Agriculture, Food and Environment, Institute of Plant Sciences and Genetics in Agriculture, The Hebrew University of Jerusalem, Rehovot 7610001, Israel
[b] Group of Agrophysics Studies, Department of Plant Sciences, MIGAL - Galilee Research Institute, Kiryat Shemona 11016, Israel

ARTICLE INFO

Keywords:
High throughput
Functional phenotyping
Tomato
S. licopersicum, Spectroradiometer
Solar induced fluorescence
Vegetation Indices

ABSTRACT

There is an urgent need to address the escalating impacts of climate change, particularly the exacerbation of drought conditions, which pose significant threats to global food security and agricultural sustainability. Innovative solutions are imperative, and one such solution involves integrating advanced technologies like the "PlantArray" system to monitor and enhance plant physiological responses to water scarcity. The "PlantArray" system enables the precise measurement of critical whole-plant physiological traits such as transpiration rate, canopy stomatal conductance, and growth rate with an exceptional spatiotemporal resolution. Augmenting this system with photosynthesis measurements offers an additional layer of information, facilitating a more focused interpretation of the system parameters. To overcome the limitations of single-leaf photosynthesis measurement techniques, this study employs a remote sensing approach to rapidly scan numerous samples at multiple time points, revealing insights into drought stress responses of *S. licopersicum* lines. An ultra-spectral spectroradiometer mounted on a mobile cart was positioned above an experimental matrix comprising drought-stressed *S. licopersicum* obsolete and mutagenic lines. Our findings reveal that the vegetation index Photochemical Reflectance Index (PRI) exhibited greater sensitivity to drought stress compared to other vegetation and photosynthesis remote sensing indices. Photosynthesis indices demonstrated increased sensitivity to daily biomass accumulation and served as predictors of final plant yield. Interestingly, Solar-Induced Fluorescence (SIF) parameters, solely indicative of photosynthesis-emitted fluorescence, exhibited no correlation with stress levels or final biomass production. This study articulates the potential to monitor plant responses to agricultural stressors through real-time physiological tracking across complete diel cycles, thereby enriching our understanding of plant-environment interactions. Ultimately, this integrated system shows promise in screening and developing crop cultivars with ideal physiological and photosynthetic traits, vital to cultivating resilient crops in extreme droughts and weather conditions.

Introduction

With increase in climate change effects, food producers are experiencing greater competition for land, water, and energy [1]. One of the most pressing challenges the crop production industry faces, is increasing drought events. Generally, drought stress occurs when soil water availability becomes a limiting factor for transpiration and gas exchange between the leaf and the atmosphere [2]. Thus, a good way to sense if the plant is under water stress is to check the variation in stomatal conductance which controls both transpiration rate and the uptake rate of CO_2 into the leaf, and therefore its photosynthetic rate. In the past century, efforts were made to develop instruments that can scan plant traits in a short period of time in order to overcome limitations of measuring many plants in field conditions. One such technology is the "PlantArray" system which is a novel high-throughput functional phenotyping system capable of measuring key whole-plant physiological traits such as transpiration rate, canopy conductance (Gs canopy) and growth rate at high spatiotemporal resolution [3]. However, achieving consistent and reproducible measurements of CO_2 exchange between the plant and its surroundings is time-consuming, rendering it impractical for screening large number of plants [4]. Chlorophyll Fluorescence (ChlF) emitted from the photosynthetic apparatus is another candidate for plant screening, since ChlF reports directly on photosynthetic

* Corresponding author.
E-mail address: oded.liran@ocean.org.il (O. Liran).
[1] Current address: Kinneret Limnological Laboratory, Israel Oceanographic & Limnological Research, P.O.Box 447, Migdal 14950, Israel

https://doi.org/10.1016/j.atech.2024.100642
Received 1 September 2024; Received in revised form 5 November 2024; Accepted 5 November 2024
Available online 8 November 2024

Acronyms

Gs	Stomatal Conductance
ChlF	Chlorophyl a Fluorescence
SIF	Solar Induced Fluorescence
RS-ETRi	Remote Sensing of Electron Transport Rate index
PSII	PhotoSystem II
PPFD	Photosynthetic Photon Flux Density
VPD	Vapor Pressure Deficit
Rh	Relative humidity
DAT	Days After Transplanting
FPP	Functional Phenotyping Platform
DMSO	DiMethyl SulfOxide
VIS	Visual range of electromagnetic spectrum
NIR	Near Infra Red range of electromagnetic spectrum
NIST	National Institute of Standards and Technology
VI	Vegetation Index
PAR	Photosynthetically Active Radiation
HSD	Honestly Significant Difference
ANOVA	ANalysis Of VAriance
WT	Wild Type
WUE	Water Use Efficiency
VWC	Volumetric Water Content
NDRE	Normalized Differential Red Edge
PRI	Photochemical Reflectance Index
PSNDC	Pigment Specific Normalized Difference (Carotenoids)
VREI2	Vogelmann Red Edge Index 2

efficiency and indirectly on photosynthetic activity and biomass production [5]. In order to perform a direct measurement, the sampled leaf or examined area should be covered, which limits the number of measurements that can be taken in a short period of time. In addition, the measurement is semi-invasive which changes the conditions of the sampled area when compared to the rest of the plant. Moreover, the direct measurements acquire information from a small area of one leaf out of the whole plant, and therefore misses information in the spatio-temporal scale [6]. A new wave of developments enables the measurement of ChlF from remote-sensing platforms [7]. The remote sensing of ChlF is based on the passive acquisition of Solar-Induced chlorophyll Fluorescence (SIF) [8]. SIF was shown to correlate well with gross primary production on a very low spatial resolution of continents [9], but when spatial resolution increases, there is a dissociation of the SIF from primary production [10]. Liran, et al. [11] suggested a new spectral index which is based on SIF and correlates with electron transport rate of PSII in plants in order to bypass the high spatial resolution dissociation problem. Further, Liran [12] shows that this Remote Sensing of Electron Transport Rate (RS-ETRi) interprets the fluorescence emission as quantum yield of Photo System II (PSII) of the measured crop, thus relating photochemistry to SIF properties. Only few works have tried to link SIF with water status-related traits [13,14]. Several studies have investigated the response of SIF to water stress and the predominant findings suggest that reduced photosynthetic efficiency and increased non-photochemical quenching lead to a decline in the emission of fluorescence in response to water stress [15,16,14].

This study aims to integrate ChlF based remote sensing indices into the "Plant-array" high throughput functional phenotyping system in order to expand its capabilities. The experimental matrix included three lines of tomato (*S. licopersicum*) -commercial, drought sensitive and drought tolerant lines. Our approach reveals new information about the relationship between ChlF based indices and the functional response of plants to natural and stress conditions.

Materials and methods

The study was conducted between May 2019 and June 2021 at the Robert H. Smith Faculty of Agriculture, Food and Environment of the Hebrew University of Jerusalem, in Rehovot, Israel. The experiments were carried out in the iCORE functional-phenotyping greenhouse (https://plantscience.agri.huji.ac.il/icore-center). The Photosynthetic Photon Flux Density (PPFD), temperature (T), vapor pressure deficit (VPD) and relative humidity (Rh) were continuously monitored during the experimental period (Table 1).

Devices and systems

The study employed PlantArray 3.0 system (PlantDitech, Yavne, Israel), a high-throughput, gravimetric-based Functional-Phenotyping Platform (FPP). Essentially, a multi sensor system is able to record soil Volumetric Water Content (VWC), water incoming and outgoing from each pot, which is situated over a load-cell. The system performed continuous and simultaneous measurements of the whole-plant daily transpiration, transpiration-rate, canopy conductance, soil water content, plant biomass gain, and Water Use Efficiency (WUE) parameters, following methodologies from Halperin and colleagues [17]. The water

Table 1
Weekly averaged meteorological parameters within the green house used in the study. PPFD – Photosynthetic Photon Flux Density; Rh – Relative humidity; VPD – Vapor Pressure Deficit; DAT – Days after Transplanting. Each value represents an average and error is the standard error of the mean.

	Date	10.5.21–16.5.21	17.5.21 – 23.5.21	24.5.21 – 30.5.21	31.5.21–7.6.21
Parameters	DAT	1–7	8–14	15–21	22–29
PPFD^{T} (μmol photons $m^{-2}s^{-1}$)	Average	321.3 ± 21.8	316.1 ± 49.5	332.9 ± 9.8	335.9 ± 19.1
	Maximum	1221.1 ± 132.8	1278 ± 87.8	1236 ± 45.8	1198 ± 51
Temperature (C^{0})	Minimum	0	0	0	0
	Average	23.4 ± 1.5	23.4 ± 1.3	24.1 ± 0.9	24.2 ± 1.1
	Maximum	31.3 ± 1.5	30.6 ± 3.0	31.9 ± 2.3	29.8 ± 1.9
RH$^{\vdash}$ (%)	Minimum	17.4 ± 3.8	18.1 ± 1.5	18.3 ± 2.3	18.4 ± 1.5
	Average	62.4 ± 2.0	62.6 ± 8.4	63.1 ± 7.6	58.8 ± 2.9
	Maximum	86.1 ± 2.6	85.2 ± 6.5	86.4 ± 2.7	80.7 ± 5.7
VPD$^{\circ}$ (kPa)	Minimum	32.1 ± 6.7	36 ± 5.3	31.1 ± 11.3	34.4 ± 6.1
	Average	1.2 ± 0.1	1.2 ± 0.1	1.2 ± 0.2	1.3 ± 0.1
	Maximum	3.1 ± 0.3	2.8 ± 0.4	3.2 ± 1.0	2.7 ± 0.1
	Minimum	0.3 ± 0.1	0.2 ± 0.3	0.1 ± 0.5	0.3 ± 0.4

T Photosynthetic Photon Flux Density.
⊢ Relative Humidity.
ɔ Vapor Pressure Deficit.

related measurement in general and in particular the canopy stomatal conductance was tested and proven to be accurate ([18], doi: 10.3389/fpls.2021.634311). The experimental setup, nutrient solutions, and system configurations are elaborately documented [3].

Plant material

Tomato (*S. lycopersicum*) introgression lines (Ils), developed by crossing the M82 cultivar and the wild-type *S. pennellii,* were used. Each of the lines contained a single homozygous restriction fragment-length polymorphism of a *S. pennellii* chromosome segment [19]. The seeds were kindly provided by Prof. Dani Zamir of the Hebrew University of Jerusalem. Based on previous work, we selected two representative lines from the Ils population for use in the main experiment. Line IL5–2 is a high-yielding, high-biomass line that outperforms the reference cultivar M82 under both optimal irrigation and drought stress conditions. This line is characterized by its high resilience, facilitating recovery from stress, making it an ideotypic line (Ideotype). The other line is IL8–1–1, exhibits susceptible performance, resulting in lower yield and biomass under optimal irrigation conditions, where under drought stress, it maintains medium biomass, indicating moderate resilience. This line's performance under stress does not reach the high productivity levels of IL5–2, reflecting its different physiological makeup and response strategies to environmental stress [20]. The experimental setup included a randomized matrix of plants from the three cultivars (one commercial cultivar + two Introgression lines) each included six biological repeats and 18 overall different plants.

Course of the experiment

The experiment included three periods:

1. A **pre-treatment** which was identical to the control group, took eight days period during which all the plants were well-irrigated, receiving six pulses of water during the night (between 20:30 and 02:30) only, to allow a proper measurement of the daily transpiration. Irrigation was applied in such a way that water was supplied in excess to ensure a complete saturation of the growing medium, with the surplus water draining through the drainage holes at the base of each pot. During that period, the FPP calculated the water-use efficiency of the plants, a value that was then used to estimate the weight of the plants in real time during the drought treatment. All the plants received the same pre-treatment regardless of which is going to receive drought treatment in the following stage.
2. A **drought treatment**. To establish a standardized drought treatment for all plants, regardless of their individual transpiration levels, precise transpiration-irrigation feedback control was automatically implemented via the PlantArray system. The dehydration rate was gradually adjusted as the drought developed, where plants were given water in deficit to the amount of water transpired in the previous day; thus, higher transpiring plants received more water to ensure a similar dehydration rate. A constant deficit volume was utilized to avoid providing a lesser deficit for plants that reduce their transpiration, resulting in a constant exacerbating deficit over time. The deficit irrigation continued until transpiration was stopped entirely for 2 days and the plants wilted. The first three days of the drought period were given a deficit of 70 mL per day, and when it was observed that the plants did not respond to this volume, the deficit was increased to 90 mL per day for the remainder of the 9 days of the experiment. Overall, the drought period lasted 12 days. This approach successfully provided a consistent progression of drought stress (the depletion of volumetric soil water content) across all plants.
3. A **recovery** period of 11 days, during which the drought-treated plants recovered from water stress and were irrigated as follows: The drought-treated plants received increased irrigation with 10 pulses of water, 2–4 minutes each. Afterwards, they received the same irrigation as the control-group plants.

Measurement of chlorophyll concentrations

Chlorophyll concentrations in leaf samples were measured three times during the experimental period, once during each of the three different phases of the experiment: pre-treatment, drought and recovery. A chlorophyll-extraction protocol with DiMethylSulfOxide (DMSO) (>99.7 %, Thermo Fisher Scientific, Waltham, Massachusets, USA) was used to calculate chlorophyll concentrations. The extraction protocol included collecting five 0.5-cm discs from the youngest mature leaf of each plant and storing the collected tissue at −76 °C for at least 24 h [21]. Each frozen sample was then combined with 2 mL DMSO and incubated in 50 °C water for 2 h [22]. After incubation, the absorbance spectrum between 400 and 800 nm was measured by a multimode microplate reader (Tecan Spark, Tecan, Switzerland) for 200 μL of each sample. Concentrations of chlorophyll a and chlorophyll b were calculated based on the equations described [23].

Acquisition of spectral information

Two sets of custom ultra-sensitivity VIS-NIR spectrometers were used in this study (Maya 2000 Pro, Ocean Insight, Orlando, Florida, USA). The spectrometers obtain a slit size of 5 μm and grating of 600 lines/mm and were calibrated with a NIST-standardized halogen light (HL-2000-LL, Ocean Insight, Orlando, Florida, USA). The wavelength range of both spectrometers was 400 nm to 838 nm and the spectral resolution was 0.32 nm (2064 values in each acquisition). The two sets were designated as a MEASUREMENT and REFERENCE units. MEASUREMENT spectrometer was coupled with an optical bare fiber with a core diameter of 400 μm and was positioned downwards at Nadir. The optical fibre was placed at a distance of about 20–40 cm from the canopy, which allowed the capture of a circular area about 8.8–17.6 cm in diameter, which suited the center of a single plant canopy. The REFERENCE spectrometer was positioned upward to measure the downwelling irradiance from the sun (diffuse plus direct beam radiation). To do that, the optical fibre was coupled with a cosine corrector optical diffuser (CC-S-DIFFUSE Spectralon Diffuser, Labsphere, Inc., NH, USA) to expand the field of view to 180°. Spectral data of each plant was taken in an experimental array at midday (between 12:00 to 13:00), 12 times over the course of the experimental period. The time of day was selected to match the time of maximum transpiration of the plants. Overall, there were two measuring points during the pre-treatment phase, six measuring points during the drought phase and four measuring points during the recovery phase. To measure all plants in a short time, a polypropylene cart with a custom-made adjustable arm was constructed on which the two spectrometers were mounted and connected to a laptop computer (Supplemental Fig. 1). The arm allowed to raise and lower the spectrometers as needed in order to track the canopy of a plant as the plant height was increased with growth.

Extraction of spectral information

Spectral information in machine units was extracted from the two spectrometer sets and converted to radiance in energy units as described in Vitrack-tamam et al. [24]. Essentially, spectra were converted using the formulation:

$$R\left(\mu W{\cdot}cm^{-2}{\cdot}sr^{-1}{\cdot}nm^{-1}\right)=\frac{(\mathrm{I}_{\lambda}-\mathrm{D}_{\lambda})[\mathrm{counts}]\cdot \mathrm{V}_{\lambda}\ [\mu \mathrm{J}\cdot \mathrm{count}^{-1}]}{\mathrm{A}[\mathrm{cm}^2]\cdot \Omega[\mathrm{sr}]\cdot \mathrm{t}[\mathrm{s}]\cdot \mathrm{b}[\mathrm{nm}]} \quad (1)$$

where, R is the light flux radiance incoming to or upwelling from the target, I_λ is the photon counts in each wavelength, D_λ is the dark current values in each wavelength [25], V_λ is the calibration vector of the spectroradiometer, A is the area from which photons are returning into

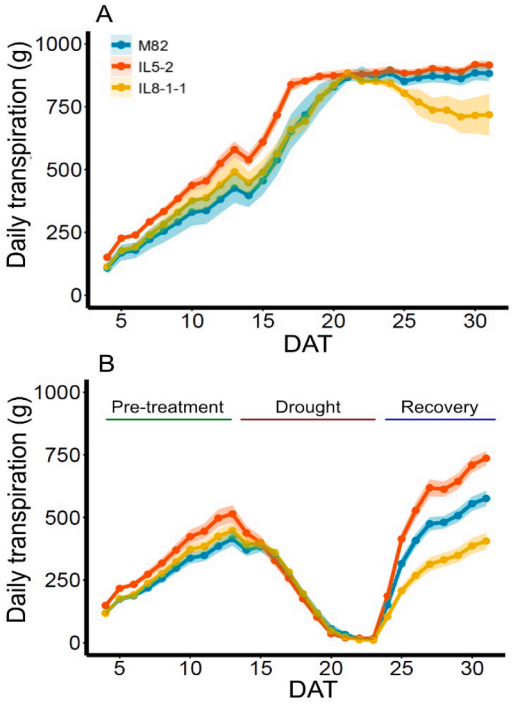

Fig. 1. (A) and (B) Daily transpiration measured with the two irrigation plans for control and drought experiment, respectively. (B) The panel is divided into three parts (colored horizontal lines) – green, red and blue that present the three irrigation treatments during the drought experiment- pre-treatment, drought, and recovery (read experiment setup section in Materials and Methods). Three colors represent the cultivars used in the study: M82 (Blue), IL5–2 (Orange), IL8–1–1 (Yellow). Each point on the curve represent $n = 4$ for control and $n = 12$ for drought experiment, and shaded areas represent standard error of the mean.

the pupil of the spectroradiometer, Ω is the solid angle of the cone from which photons are collected, t is the integration time selected during a single acquisition, and b is the bandpass, the spectral width between two successive wavelengths in the recorded spectrum. Normalized reflectance spectrum was created by ratio of MEASUREMENT and REFERENCE spectra and corrected to solar position and distance from earth according to Gordon and Wang [26].

Calculation of vegetation indices (VIs)

VIs were calculated according to the formulations listed in (Table 2).

Statistical analysis

The data analysis was performed using the JMP ver. 15.0 (SAS Institute INC., NC, USA) statistical package and Excel (Microsoft, WA, USA). In all of the comparison tests, groups were checked for normal distribution with the Shapiro–Wilk's test and the homogeneity of variance with Levene's test. If both tests were satisfied, *t*-test was used to compare two groups, and ANalysis Of Variance (ANOVA) compare several groups. Tukey's Honestly Significant Difference (HSD) was used for multiple comparisons *post-hoc*. When comparing to a control group, Dunnett's test was used. If the normality criteria were violated, Wilcoxon/Kruskal–Wallis's nonparametric ANOVA was used, with Wilcoxon pair *U test* for multiple comparisons post-hoc. All tests were performed at a significance level of at least $\alpha < 0.05$. The mean values for all results are presented with ± S.E. The squared values of Pearson correlation coefficients were also calculated in regression analyses. The graphs were plotted using Microsoft Excel 2019. Correlation plots were calculated using R language.

Results

Ultra-sensitive spectroradiometers were installed on a specially designed trolley, featuring an arm that placed above an experimental array of *S. licopersicum* plants comprising three different lineages (**Supplement Figure 1A**). The spectroradiometer and its fiber optic is positioned at Nadir above the plants (**Supplement Figure 1B**). The planned experiment included two groups of plants– control and drought (Fig. 1**A and 1 B,** respectively). The control group shows that daily transpiration increased in the first 20 days in the three cultivars with the drought ideotype cultivar IL5–2 transpired more than the WT and the drought susceptible cultivars (Fig. 1**A**). It also reached a plateau in transpiration earlier than the two other cultivars. The drought susceptible cultivar declined its maximum transpiration rate after reaching maximum, unlike the other two cultivars, albeit not statistically significant difference. The fact that only the drought susceptible cultivar shows a larger deviation towards the end of the control period, behaves as expected, given its poor vigor, stunted growth and reduced vitality [32]. The drought treatment shows that daily transpiration decreased similarly in all varieties during the 12 days of the drought dehydration treatment (Fig. 1**B**). Daily transpiration of all varieties commenced and increased once irrigation was turned on in the recovery period. The

Table 2
Vegetation indices calculated in this study. NDRE – Normalized Differential Red Edge index; PRI – Photosynthesis Response Index; PSNDc- Pigment Specific Normalized Difference (carotenoids); VREI2 – Vogelmann Red Edge Index 2; NDVI- Normalized Differential Vegetation Index; SIF- Solar Induced Fluorescence; RS-ETRi – Remote Sensing of Electron Transport Rate index.

#	Index	Wavelength	Meaning	Formulation	Reference
1	NDRE	720, 790	Amount of chlorophyll in plants	$\frac{\rho_{790}-\rho_{720}}{\rho_{790}+\rho_{720}}$	Barnes et al. [27]
2	PRI	531,570	Amount of xanthophylls of stress in plants	$\frac{\rho_{531}-\rho_{570}}{\rho_{531}+\rho_{570}}$	Gamon 1992
3	PSNDc	800, 470	Amount of carotenoids in plants	$\frac{\rho_{800}-\rho_{470}}{\rho_{800}+\rho_{470}}$	Blackburn GA, [28]
4	VREI2	734, 747, 715, 726	Water amount normalized to leaf area	$\frac{\rho_{734}-\rho_{747}}{\rho_{715}+\rho_{726}}$	Vogelmann JB, [29]
5	NDVI	680, 800	Plant structure	$\frac{\rho_{800}-\rho_{680}}{\rho_{800}+\rho_{680}}$	[30]
6	SIF_{687},SIF_{760}	686.7, 686.8, 757.6, 759.3	Fluorescence emission out of PSII or PSI[Δ]	$\frac{\alpha_R \cdot I_{out} \cdot I_{in} - I_{in} \cdot L_{out}}{\alpha_R \cdot I_{out} - \alpha_F \cdot I_{in}}$	Alonso, [31]
7	RS-ETRi	680, 800, 686.7, 686.8, 757.6, 759.3	Electron transport rate out of PSII	$PAR \cdot NDVI \cdot \frac{SIF_{687} - SIF_{760}}{SIF_{687}}$	Liran, [11]

[Δ] $\alpha_R = \frac{R_{out}}{R_{in}}; \alpha_F = \frac{f_{out}}{f_{in}}.$

three varieties respond differently to commence of irrigation according to their physiological properties (Fig. 1**B**), where the drought ideotype cultivar transpiring the fastest and drought susceptible cultivar the slowest. The final point of daily transpiration rate was also found in a gradient with respect to the cultivars identities where the highest rate achieved by the drought ideotype cultivar (Notice how the curves are placed at DAT 31). At the last day of the measurement (DAT 31), Dry weight of the biomass and fruit (gr), Water Use Efficiency (WUE) (gr/ml), transpiration (gr) and Gs canopy (gr/gr*min) were measured (Fig. 2).

There was a distinct difference between the control and drought groups for each cultivar in the case of dry weight, where the lines in the drought group were significantly lower than the control (Fig. 2**A**). WUE was lower during drought period for the M82 cultivar and the drought ideotype cultivar relative to the control, but remained unchanged in the drought susceptible cultivar, as expected (Fig. 2**B**). Daily transpiration showed statistically significant differences in the various cultivars (Fig. 2**C**), where the drought sensitive cultivar transpired the least of the three and as compared to the control. Gas exchange of the canopy showed trends of difference between the control and drought group, albeit non-significant (Fig. 2**D**). Reflectance spectra in the control and drought groups differ mostly in the height of the reflectance between 680 nm and 800 nm (Fig. 3**A and 3 B, respectively**).

Visual subtle changes in the spectra between cultivars included the following electromagnetic spectrum ranges: 400 nm – 500 nm, 530 nm-570 nm (chlorophyll peak), 702 nm- 750 nm (Red Edge range), 790 nm-820 nm (mesophyll plateau). Differences in the reflectance power between cultivars was opposite between control and drought groups (Fig. 3**A and 3 B**, respectively). In the control (Fig. 3**A**), drought susceptible cultivar IL8–1–1 reflectance spectrum was slightly higher than the drought ideotype cultivar IL5–2 and higher than M82 cultivar, especially at the near infrared region (790 nm-820 nm). This trend flips and narrowed for the reflectance averaged over the drought treatments. In order to grasp on the differences of the spectra between the control and drought treatments, several Vegetation Indices (VIs) and ChlF related indices were calculated on the spectra acquired along the experimental period (See Table 2 Materials and Methods). Correlation analysis was performed between the plant characteristics and known Vegetation Indices (VIs) in order to search for meaningful information between optical properties and the physiology of the plant. Correlation analysis was performed twice, between chlorophyll a and b to vegetation, and to photosynthesis related indices (Fig. 4 **and** Fig. 5**, respectively**). The analysis was performed on the averages of each treatment for three experimental dates: DAT 14, 21 and 28, i.e. at the onset of drought, during the maximum drought stress manifestation and two days after full recovery from the drought stress. Transpiration rate and daily transpiration were highly correlated as expected (Fig. 4). Chlorophyll a and b were moderately negatively correlated with PRI index which implies for a photosynthetic stress which reduces the amount of active photosystems, as expected. Daily transpiration was highly correlated with NDVI index which relates to biomass production. The same set of phenotyping indices was correlated with ChlF related indices (Fig. 5). SIF_{687} and SIF_{760} were only slightly negative related to the pigments, as expected. This is because with more chlorophylls found, the chance for more active photosynthetic units is higher, therefore less fluorescence would escape the canopy and reach the detector. Chlorophyll a was correlated better than Chlorophyll b with the RS-ETRi index which senses electron transport rate on the canopy, as expected. This is

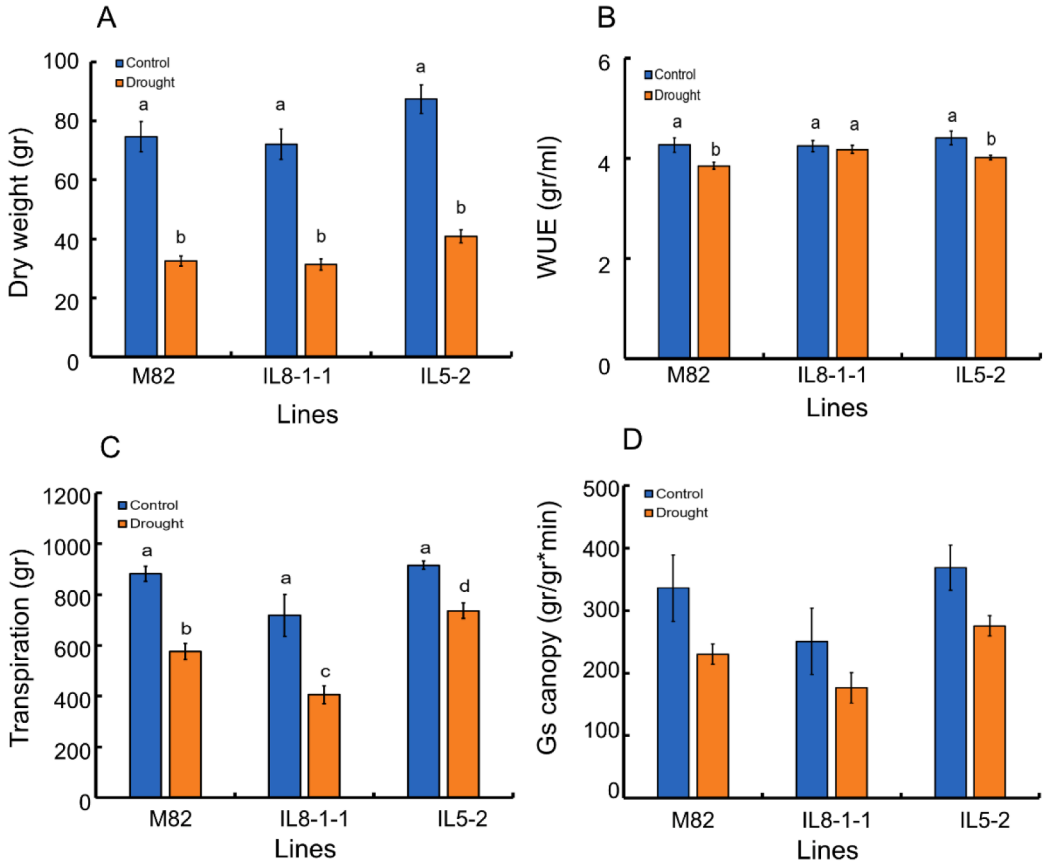

Fig. 2. Plant parameters at the end of the experimental period. (A), (B), (C) and (D) are Dry weight (gr) Water Use Efficiency (WUE) in (mgr), Daily transpiration in (gr) and Gs canopy in gram water to gram plant to minutes. Two groups Control and Drought are Blue and Orange, respectively. Each column represents an average of the experimental group with $n = 4$ for control and $n = 12$ for drought. Error bars are standard error of the mean (S.E.). Letter annotations present statistically significant at $p < 0.0001$ for Panel (A), $p < 0.05$ for Panel (B) and $p < 0.05$ for Panel (C).

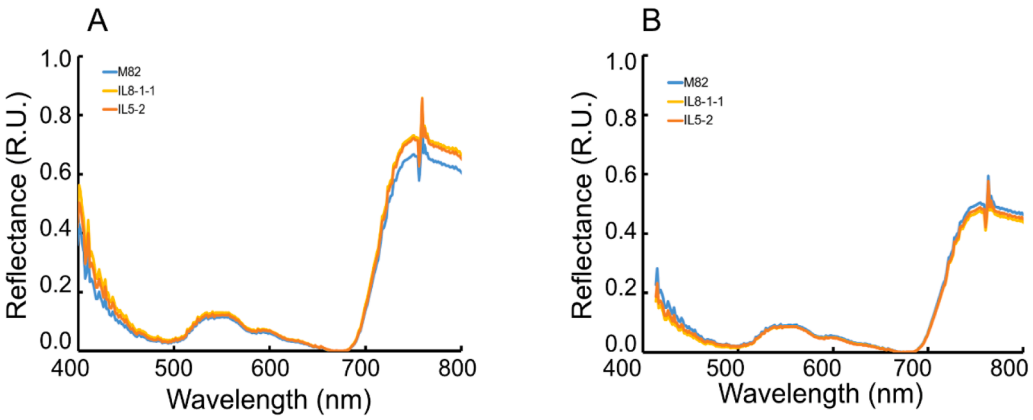

Fig. 3. Reflectance spectra of tomato *S. licopersicum* potted plants in the control (A) and drought (B conditions. Spectra shown were acquired DAT 24 where irrigation level reach minimum according to the experimental plan. Each curve represents a different cultivar of the tomato, where blue, yellow and orange colors represent cultivars M82, IL8–1–1 and IL5–2, respectively. Each curve is an average of 4 biological repeats and 12 biological repeats in the case of control and drought groups, respectively. Spectra were double normalized in order to keep the rate of change between 0 and 1 on the reflectance axis.

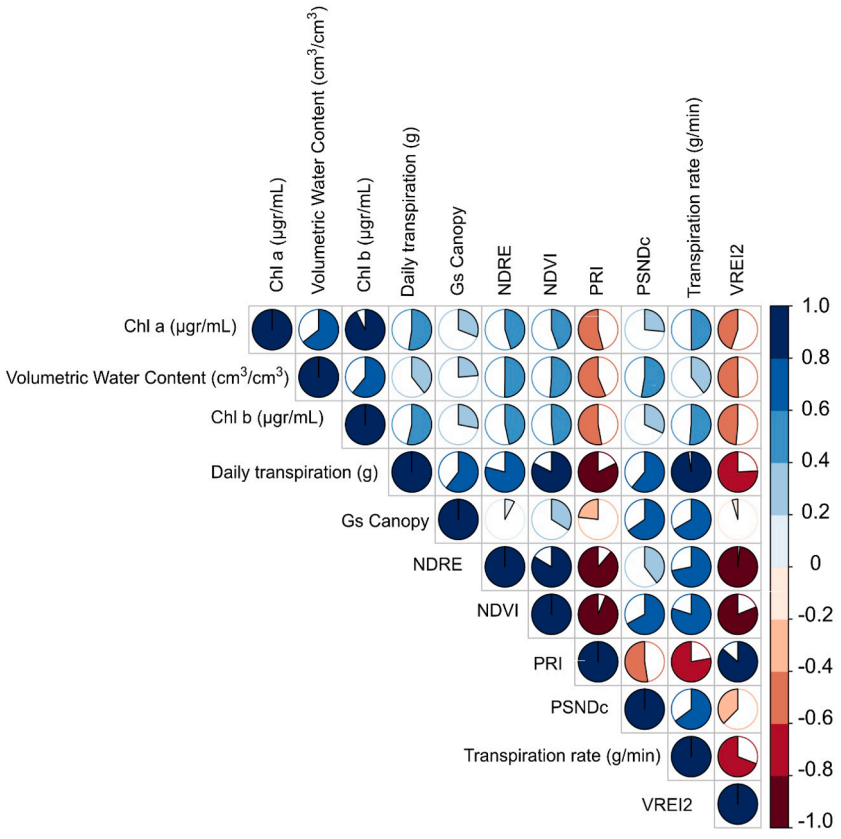

Fig. 4. Correlation analysis between physiological parameters and vegetation indices in *S. licopersicum*. Blue and red colors represent positive and negative correlation, respectively. The fill fraction presents visually the strength of the correlation, where for positive values, the circle is filled clockwise and for negative values, it is filled counter clockwise. Data was checked for monotonous relationship, and normal distribution. Correlation was calculated on averages of values for each cultivar and experimental setup -drought and control. Acronyms represent NDRE – Normalized Differential Red Edge index; PRI – Photochemical Reflectance Index; PSNDc- Pigment Specific Normalized Difference (carotenoids); VREI2 – Vogelmann Red Edge Index 2; NDVI- Normalized Differential Vegetation Index. $n = 12$.

because chlorophyll a is the central pigment found in the photosystems, and higher concentration of it implies for higher number of active photosystems. Chlorophyll b, on the other hand, is an accessory pigment which is found only in the light harvesting complexes of the photosystems. RS-ETRi correlated moderately and positively with the soil volumetric water content and daily transpiration as would be expected in view of a healthy plant which transpires when performing photosynthesis.

We were interested to track the time dependent differences between cultivars on the background of soil moisture during drought treatment (Fig. 6). We selected several representative VIs: Normalized Differential Red Edge (NDRE) and Vogelman Red Edge Index 2 (VREI2) for the red edge region; Photochemical Reflectance Index (PRI) for the 530 nm – 570 nm, Pigment Specific Normalized Difference (carotenoids) (PSNDc) for the two limits of the spectral range (470 nm and 800 nm) acquired in the study; Solar Induced Fluorescence (SIF) for the Fraunhofer lines at

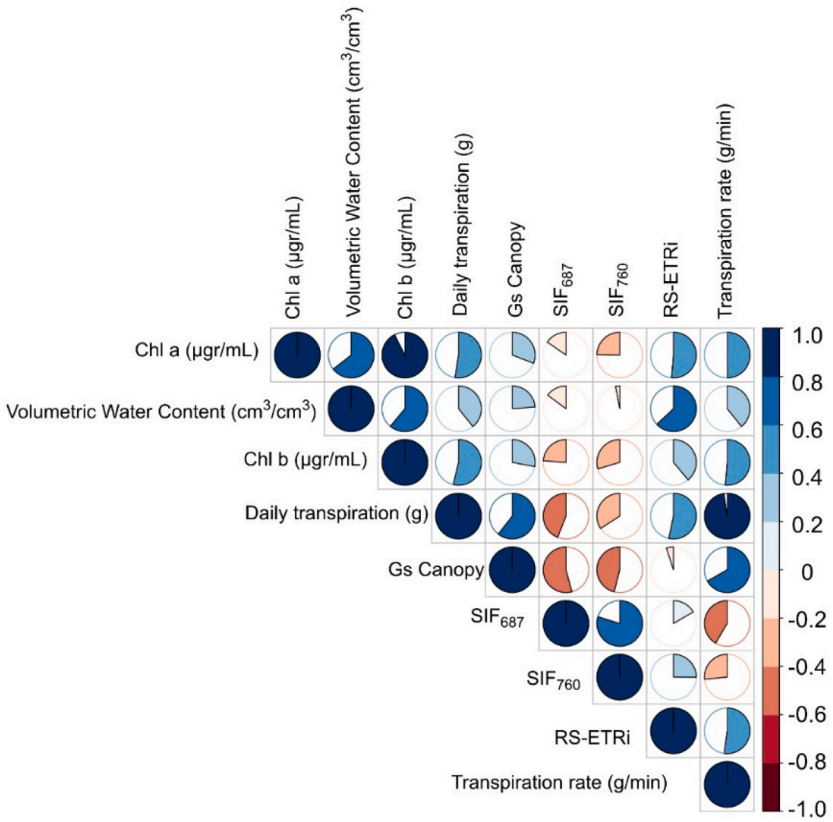

Fig. 5. Correlation analysis between Physiological parameters and photosynthesis-based indices in *S. licopersicum*. Blue and red colors represent positive and negative correlation, respectively. The fill fraction presents visually the strength of the correlation, where for positive values, the circle is filled clockwise and for negative values, it is filled counter clockwise. Data was checked for monotonous relationship, and normal distribution. Correlation was calculated on averages of values for each cultivar and experimental setup -drought and control. Acronym represent SIF- Solar Induced Fluorescence; RS-ETRi – Remote Sensing of Electron Transport Rate index.
$n = 12$.

687 nm and 760 nm and Remote Sensing of Electron Transport Rate index (RS-ETRi) which approximates electron transport rate on the thylakoid membranes within the chloroplast. The ratio between the drought and control values was more informative and showed better response to the physiology of the plant. Therefore, each curve in the panels is the normalized response of the drought group to that of the control group. In general, along the experimental period, the most varied region of response for both the VIs and ChlF related indices was during the start of the recovery period from drought at DAT 23. Both drought sensitive and drought tolerant strains showed a higher Volumetric Water Content (VWC) before and after the drought period when compared to the M82 cultivar (Fig. 6, all panels, the light grey curves). M82 VIs and the SIF indices were not so sensitive to the decline in VWC along the drought period (Fig. 6**A, 6 B**). They started to respond to the drought only during DAT 20, about a week after the start of the drought period. PRI showed a decline in the signal (Orange line Fig. 6**A**) which started even before the inflicted drought event. The rate of decrease in the signal got stronger with the development of the water stress. RS-ETRi also responded to the drought in the same manner but with a smaller amplitude. The PSNDc and the RS-ETRi responded immediately to the recovery of the plant, whereas the other VIs responded slower -PRI started to increase only 1 day later (Fig. 6**A,** orange line), red edge related indices NDRE and VREI2 took the rest of the experimental period to recover (Fig. 6**A**, Magenta and Purple lines) and SIF indices (Fig. 6**B,** green lines) did not respond at all to the drought period. The behavior of the VIs to drought in the case of the drought ideotype cultivar IL5–2 (Fig. 6**C**) was similar to that of the M82, except here all the VIs declines along the experimental period with an increase in decline rate during the drought period. Again, the PSNDc response to recovery was faster than that of the PRI that responded only the following day. The SIF signals increased during the drought period in the case of the drought ideotype cultivar IL5–2 (Fig. 6**D**), albeit not statistically significant, implying that the apparatus of this cultivar may respond differently to the inflicted stress. The fluorescence signal relaxed after the drought period ended, however it took it the rest of the experimental period to recover. RS-ETRi responded only towards the end of the drought period at DAT 20, one week after the start of the stress (Fig. 6**D**, blue line). In the case of the drought susceptible cultivar IL8–1–1, the response trend of the VIs is similar to the M82 trend along the development of the drought stress in the plant (Fig. 6**E**), where all the VIs response are lagged in one day after the recovery started, but the response is pronounced and much sharper than both the M82 and the IL5–2 cultivars. SIF indices in these cultivars are the only ones that respond to the recovery phase (Fig. 6**F**, green and light green lines). However, the drought event itself was unnoticed, rather the recovery event elicited a sharp response (Fig. 6**F**, the dip in the line for both green colors during DAT24 and forward).

We were also interested to see if the calculated VIs and photosynthetic indices correlate with a change in plant weight along the experiment (Fig. 7).

Optical VIs were correlated in general with the daily plant weight, while the SIF indices showed no response. Regarding the VIs (Fig. 7**A** and **7 C** for control and drought groups, respectively), Data show higher correlation for the control treatment than the drought treatment. The highest correlation was found for NDRE index (Fig. 7**A**, Magenta color) with R^2=0.79 correlated with the daily plant weight. PRI and PSNDc indices (Fig. 7**A**, orange and yellow colors, respectively) were much less correlated to daily plant weight, as would be expected because they are related to pigments and not directly to primary productivity. Plants that

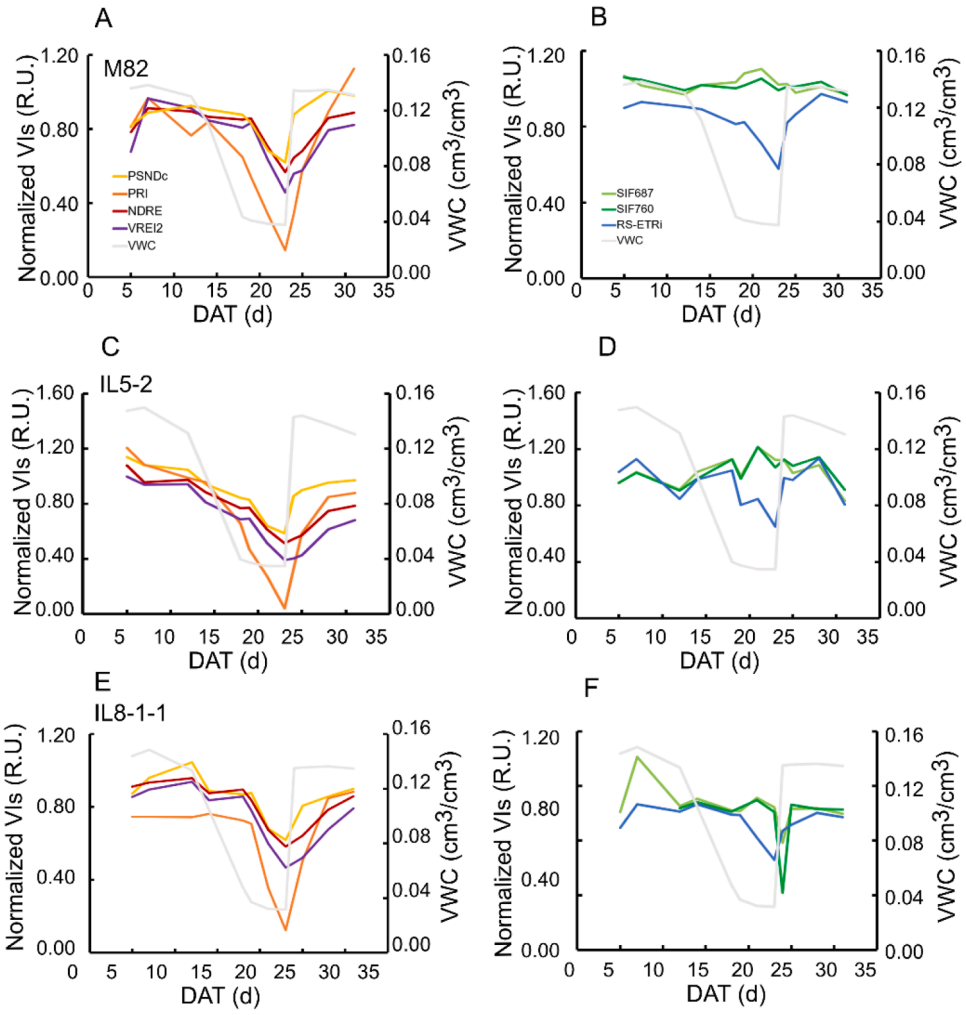

Fig. 6. Normalized vegetation and photosynthesis related indices performance along the study. Panels (A), (C) and (E) represent vegetation indices calculated directly from the spectra, and (B), (D) and (F) represent Solar Induced Fluorescence (SIF) based indices calculated from the Fraunhofer absorption lines. Drought information was averaged per group and index and was normalized to the average control information in each time point along the study. Soil Volumetric Water Content (VWC) is given for each cultivar in light grey as a reference to the actual behavior of the group measured. Colors for each index in all the panels are given in the legend in Panel (A) and (B) for the vegetation indices and photosynthesis related indices, respectively.

experienced drought show a decline in the correlation between the daily weight and VIs (Fig. 7**C**). Photosynthesis related indices were not sensitive to the variation in the daily weight in both the control and the drought treatments (Fig. 7**B, 7 E**, respectively). $SIF_{687,760}$ don't show any response to the daily weight, and RS-ETRi shows a very weak and sparsely distributed relationship, as would be expected from a primary production related index.

Finally, it was asked whether VIs and photosynthesis related indices measured along the experimental period will be able to correlate to the final biomass achieved at the end of the experiment, that is shoot+fruit mass (Fig. 8). System parameters such as Gs canopy and Daily transpiration showed the highest correlation to the final produce weight at DAT 16–18 and DAT 26. It seems that starting at DAT 15, correlation starts to rise for all indices, where the peak of correlation is achieved at DAT 24. The highest correlation for the VIs and ChlF based indices achieved was between the RS-ETRi, PRI, NDRE, VREI2, PSNDc and quantum yield in ascending order. The highest correlation value for the indices was about 0.7 for the quantum yield, which is just the RS-ETRi index without the multiplication with the PPFD value (see Table 2 for explanation on the index). SIF indices showed no relationship with the final weight whatsoever.

Discussion

In this study, we explored the potential of Vegetation and SIF-based indices to provide the capacity of performing high-frequency measurements and high-throughput analysis of photosynthesis, for which conventional tools have thus far fallen short [33]. For the demonstration of the system capacity we selected three *S. licopersicum* variants that respond differently to drought (Fig. 1) [34]. Dry weight, WUE, Transpiration and Gs canopy of the drought treatments were all lower than the control (Fig. 2) as expected for these variants [34], and as shown previously in the literature for drought tolerant and sensitive species [35]. The decline in the reflectance of drought treatments (Fig. 3) is also corroborated by the literature, where spectral interferences between the cell wall and air increase in water stressed plants [36]. In addition, stressed plants demonstrated an overall decrease in pigments composition which overall results in a smaller magnitude of the optical reflectance spectrum [37]. The study checked correlation of VIs and photosynthesis-based indices with the physiology parameters and showed that photosynthetic indices were less sensitive to water stress inflicted on the plants (Fig. 4, 5). This is expected, because irrigation stress closes stomata and reduces the carbon flux into the cell which minimized in turn photosynthesis. Significant damage to the photosynthesis mechanism itself starts to present damage at a substantial

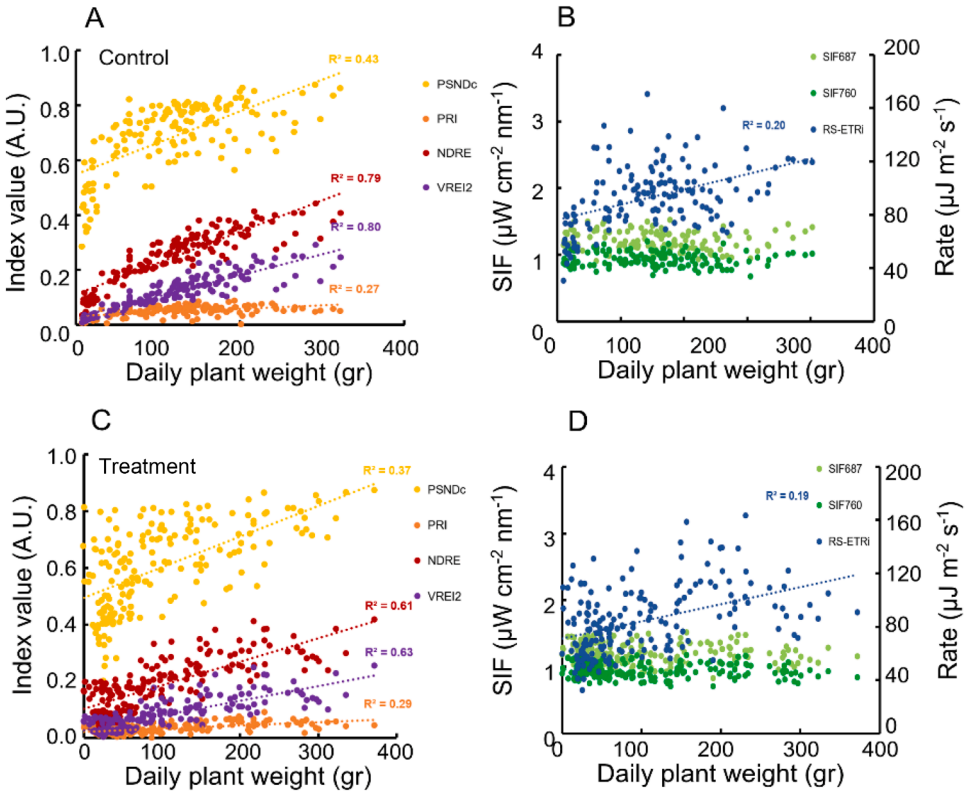

Fig. 7. Relationship between vegetation and photosynthesis related indices with daily measured plant weight. The four panels represent vegetation indices (A,C) and Photosynthesis related indices (B,D) data with the two experimental groups control (A,B) and drought (C,D). Each color represents the various indices and names are shown in the legend of each panel. Dotted line for each index represents the trend line and coefficient of determination value is shown in the respected color of the index.

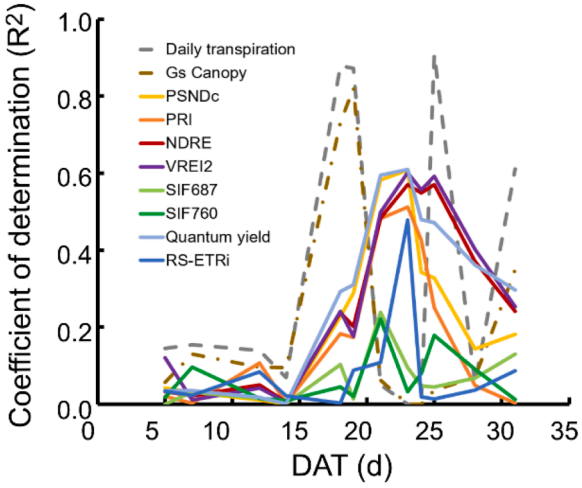

Fig. 8. Coefficient of determination calculated vegetation and photosynthesis indices and final weight. Final weight was taken as the fresh mass measured, both plant shoot, root, leaves and fruit at the end of the experiment. Each curve represents an average of all the samples in both groups – drought and control for the respected index.

longer time than visual signals such as wilting [38]. PRI is considered to be a good indicator of the level of plant water stress [39]. It is very sensitive to heat dissipation, which increases under water-stress conditions [40], and to the rapid changes in carotenoids that occur through the de-epoxidation of the xanthophyll pigments [41]. PRI decreased in values with increase in chlorphyll content in this study, as expected (Fig. 4). Increase in chlorophyl content also decreased SIF based indices as suggested by [42], due to increase in fluorescence photons re-absorption, and increase in canopy size [9].

SIF is indirectly related to photosynthetic activity in plants as it is the surplus of unused energy which is emitted back to the environment [5]. We hypothesized that SIF would be a useful remote-sensing indicator for drought stress than traditional VIs, see rational in [43]. However, our findings are opposite to the expected outcome. SIF was much less sensitive to the drought stress when compared with optical indices (Fig. 6). Specifically, PRI was very sensitive and shows a change almost from the beginning of the stress for the M82 and IL5–2 but not IL8–1–1 (Fig. 6**A, 6 B, 6 C** orange curve). Thenot F. et al. [39] state that as long as drought phenotype of wilting leaves are taken into account, PRI is indeed a reliable drought stress index. When checking how well VIs and photosynthesis related indices report on daily biomass accumulation, PRI becomes the least sensitive index for biomass production, corroborated by an additional carotenoid-based index, the PSNDc (Fig. 7). Although many studies have reported on a strong relationship between SIF and primary production [44,9], we did not find meaningful correlations between plant biomass gain and SIF_{687} or SIF_{760} (Fig. 7**B, 7 D**). This may happen because the SIF emitted during photosynthetic activity reports on the amount of energy not used for photosynthesis. But during stress, additional energy is dissipated as heat disconnecting the relationship between fluorescence emission and primary productivity [45].

Red edge-based VIs showed the highest correlation to daily plant weight in both the control and drought treatments as seen in previous studies as well, where VIs based on red edge, accurately predict primary production in maize [46] and wheat [47].

Finally, the correlations between final produce of the cultivars and remote sensing indices, could potentially aid farmers in forecasting agricultural yields using seasonal remote sensing data from their fields. We show that red edge-based vegetation indices can predict moderately the amount of biomass produce at the end of the cultivation period

(Fig. 8). There was a significant positive (logarithmic) correlation between RS-ETRi and the plant weight which is related to the logarithmic correlation between the special SIF term within this index [12], implying for complex relationship between light use efficiency and biomass production. The physiological parameters transpiration and Gs canopy were highly correlated to the final produce on DAT 16, 17 and 25 along the experiment.

Although this study did not directly validate photosynthesis measurements at the leaf level with established handheld fluorometers or gas exchange systems, we believe it significantly advances our understanding by demonstrating a direct correlation between fluorescence indices and basic plant water relation metrics. We successfully measured crucial physiological parameters such as transpiration and canopy stomatal conductance across all plants simultaneously and continuously throughout the experiment, involving a high number of biological samples in agronomic environment. To further enhance our research, we recommend incorporating measurements of effective quantum yield with hand held devices, which can be performed rapidly enough for future experiments. As our measurements were specifically conducted during early noon, as suggested by the study of Prior et al. [48], we propose that extending these measurements to various times of the day could illuminate aspects of the carbon balance and how plants manage stress throughout the diurnal cycle. Finally, addressing one of humanity's greatest challenges—developing new crop breeds capable of withstanding extreme events of droughts and weather conditions [49]—this integrated system holds promise for assisting in the screening and development of crop cultivars with optimal physiological as well as photosynthetic characteristics.

Conclusion

This study applied a remote sensing technique to detect chlorophyll a fluorescence over canopies of plants, tracked for their physiology in a high throughput functional phenotyping platform. The study shows that SIF based vegetation indices mostly relate to biomass production parameters such as daily biomass production and fruit and shoot final biomass. Reflectance based vegetation indices succeed better in detecting stress in the plant. This study lays a foundation for developing new remote sensing indices that can be tested first on single plant canopies level and later to be scaled up to large fields. The study also articulates the complementary information that can be perceived from parallel measurements of both chlorophyll a fluorescence and primary productivity measured as daily biomass gain.

Ethical statement

All procedures were performed in compliance with relevant laws and institutional guidelines

CRediT authorship contribution statement

Amir Mayo: Writing – original draft, Methodology, Investigation, Formal analysis, Data curation, Conceptualization. **Snir Vitrack-Tamam:** Writing – original draft, Software, Methodology, Investigation, Formal analysis, Data curation. **Menachem Moshelion:** Writing – review & editing, Writing – original draft, Visualization, Supervision, Project administration, Methodology, Investigation, Funding acquisition, Formal analysis, Conceptualization. **Oded Liran:** Writing – review & editing, Writing – original draft, Visualization, Supervision, Project administration, Methodology, Investigation, Funding acquisition, Data curation.

Declaration of competing interest

The authors declare no competing interests.

Acknowledgments

This research was supported by the Chief Scientist of the Israeli Ministry of Agriculture and Rural Development, Noah Ark project, Grant No. 21–37–0011 to O.L.

This research was also partly supported by the Israel Science Foundation (ISF), Grant No. 1043/20 to M.M.

Supplementary materials

Supplementary material associated with this article can be found, in the online version, at doi:10.1016/j.atech.2024.100642.

Data availability

Data supporting the findings of this study are available from the corresponding author O.L. on request.

References

[1] D. Tilman, J. Fargione, B. Wolff, C. D'Antonio, A. Dobson, R. Howarth, D. Schindler, W.H. Schlesinger, D. Simberloff, D. Swackhamer, Forecasting agriculturally driven global environmental change, Science 292 (2001) 281–284.
[2] M. Moshelion, The dichotomy of yield and drought resistance: Translation challenges from basic research to crop adaptation to climate change, EMBO reports 21 (12) (2020) e51598.
[3] A. Dalal, I. Shenhar, R. Bourstein, A. Mayo, Y. Grunwald, N. Averbuch, Z. Attia, R. Wallach, M. Moshelion, A telemetric, gravimetric platform for real-time physiological phenotyping of plant–environment interactions, JoVE J Vis Exp (2020) e61280.
[4] S.P. Long, C.J. Bernacchi, Gas exchange measurements, what can they tell us about the underlying limitations to photosynthesis? Procedures and sources of error, J. Exp. Bot. 54 (2003) 2393–2401.
[5] N.R. Baker, Chlorophyll fluorescence: a probe of photosynthesis in vivo, Annu Rev. Plant Biol. 59 (2008) 89–113.
[6] U. Schreiber, Pulse-amplitude-modulation (PAM) fluorometry and saturation pulse method: an overview, in: GC Papageorgiou, Govindjee (Eds.), Chlorophyll Fluoresc, Springer Netherlands, Dordrecht, 2004, pp. 279–319.
[7] A. Porcar-Castell, E. Tyystjärvi, J. Atherton, C. Van Der Tol, J. Flexas, E.E. Pfündel, J. Moreno, C. Frankenberg, J.A. Berry, Linking chlorophyll a fluorescence to photosynthesis for remote sensing applications: mechanisms and challenges, J. Exp. Bot. 65 (2014) 4065–4095.
[8] J.A. Plascyk, The MK II Fraunhofer line discriminator (FLD-II) for airborne and orbital remote sensing of solar-stimulated luminescence, Opt. Eng. 14 (1975) 144339.
[9] L. Guanter, Y. Zhang, M. Jung, J. Joiner, M. Voigt, J.A. Berry, C. Frankenberg, A. R. Huete, P. Zarco-Tejada, J.E. Lee, et al., Global and time-resolved monitoring of crop photosynthesis with chlorophyll fluorescence, Proc. Natl. Acad. Sci. u S. a 111 (2014) E1327–E1333.
[10] J.K. Marrs, J.S. Reblin, B.A. Logan, D.W. Allen, A.B. Reinmann, D.M. Bombard, D. Tabachnik, L.R. Hutyra, Solar-induced fluorescence does not track photosynthetic carbon assimilation following induced stomatal closure, Geophys. Res. Lett. 47 (2020) e2020GL087956.
[11] O. Liran, O.M. Shir, S. Levy, A. Grunfeld, Y. Shelly, Novel remote sensing index of electron transport rate predicts primary production and crop health in L. sativa and Z. mays, Remote Sens. 12 (11) (2020) 1718.
[12] O. Liran, Formulation of a structural equation relating remotely sensed electron transport rate index to photosynthesis activity, Remote Sens 14 (2022) 2439, 2022Page14: 2439.
[13] X. Lu, Z. Liu, S. An, D.G. Miralles, W. Maes, Y. Liu, J. Tang, Potential of solar-induced chlorophyll fluorescence to estimate transpiration in a temperate forest, Agric. For. Meteorol. 252 (2018) 75–87.
[14] S. Xu, Z. Liu, L. Zhao, H. Zhao, S. Ren, Diurnal response of sun-induced fluorescence and pri to water stress in maize using a near-surface remote sensing platform, Remote Sens 10 (2018) 1510, 2018Page10: 1510.
[15] A. Ač, Z. Malenovský, J. Olejníčková, A. Gallé, U. Rascher, G. Mohammed, Meta-analysis assessing potential of steady-state chlorophyll fluorescence for remote sensing detection of plant water, temperature and nitrogen stress, Remote Sens. Environ. 168 (2015) 420–436.
[16] S.Z. Dobrowski, J.C. Pushnik, P.J. Zarco-Tejada, S.L. Ustin, Simple reflectance indices track heat and water stress-induced changes in steady-state chlorophyll fluorescence at the canopy scale, Remote Sens. Environ. 97 (2005) 403–414.
[17] O. Halperin, A. Gebremedhin, R. Wallach, M. Moshelion, High-throughput physiological phenotyping and screening system for the characterization of plant–environment interactions, Plant J. 89 (2017) 839–850.
[18] V. Jaramillo Roman, R. van de Zedde, J. Peller, R.G. Visser, van der Linden, van Loo, High-resolution analysis of growth and transpiration of quinoa under saline conditions, Front. Plant Sci. 12 (2021) 634311.

[19] Eshed Y., Zamir D. (1995) An introgression line population of lycopersicon pennellii in the cultivated tomato enables the identification and fine mapping of yield-associated QTL.
[20] S.C. Gosa, B.A. Gebeyo, R. Patil, R. Mencia, M. Moshelion, Diurnal stomatal apertures and density ratios affect whole-canopy stomatal conductance, water-use efficiency and yield, a, bioRxiv, 2022, 2022.01.06.475121.
[21] R. Moran, Formulae for determination of chlorophyllous pigments extracted with N,N-dimethylformamide, Plant Physiol. 69 (1982) 1376.
[22] J. Novák, J. Pavlů, O. Novák, V. Nožková-Hlaváčková, M. Špundová, J. Hlavinka, Š. Koukalová, J. Skalák, M. Černý, B. Brzobohatý, High cytokinin levels induce a hypersensitive-like response in tobacco, Ann. Bot. 112 (2013) 41–55.
[23] A.R. Wellburn, The spectral determination of chlorophylls a and b, as well as total carotenoids, using various solvents with spectrophotometers of different resolution, J. Plant Physiol. 144 (1994) 307–313.
[24] S. Vitrack-Tamam, H. Yasour, D. Hamus-Cohen, R. Erel, L. Rubinovich, O. Liran, Solar induced fluorescence retrieved from avocado (*Persea americana* Mill.) Canopies along the season correlates with sugar levels in the developing fruit, bioRxiv (2023), 2023–07.
[25] A. Burkart, S. Cogliati, A. Schickling, U. Rascher, A novel UAV-based ultra-light weight spectrometer for field spectroscopy, IEEE Sens. J. 14 (1) (2013) 62–67.
[26] H.R. Gordon, M. Wang, Retrieval of water-leaving radiance and aerosol optical thickness over the oceans with SeaWiFS: a preliminary algorithm, Appl. Opt. 33 (3) (1994) 443–452.
[27] E.M. Barnes, T.R. Clarke, S.E. Richards, P.D. Colaizzi, J. Haberland, M. Kostrzewski, M.S. Moran, Coincident detection of crop water stress, nitrogen status and canopy density using ground based multispectral data, In Proceedings of the fifth international conference on precision agriculture, Bloomington, MN, USA 1619 (6) (2000).
[28] G.A. Blackburn, Quantifying chlorophylls and caroteniods at leaf and canopy scales: An evaluation of some hyperspectral approaches, Remote Sens. Environ. 66 (3) (1998) 273–285.
[29] J.E. Vogelmann, B.N. Rock, D.M. Moss, Red edge spectral measurements from sugar maple leaves, TitleRemote Sens. 14 (8) (1993) 1563–1575.
[30] Rouse J.W., Jr (1974) Monitoring the vernal advancement and retrogradation (green wave effect) of natural vegetation.
[31] L. Alonso, L. Gomez-Chova, J. Vila-Frances, J. Amoros-Lopez, L. Guanter, J. Calpe, J. Moreno, Improved fraunhofer line discrimination method for vegetation fluorescence quantification, IEEE Geosci. Remote Sens. Lett. 5 (4) (2008) 620–624.
[32] S.C. Gosa, B.A. Gebeyo, R. Patil, R. Mencia, M. Moshelion, Diurnal stomatal apertures profile and density ratios affect whole-canopy conductance, drought response, water-use efficiency and yield, b, BioRxiv, 2022, 2022–01.
[33] Fu Yingchun, Zhe Zhu, Liangyun Liu, Wenfeng Zhan, Tao He, Huangfeng Shen, Jun Zhao, et al., Remote Sensing Time Series Analysis: A Review of Data and Applications, Journal of Remote Sensing (2024).
[34] S.C. Gosa, A. Koch, I. Shenhar, J. Hirschberg, D. Zamir, M. Moshelion, The potential of dynamic physiological traits in young tomato plants to predict field-yield performance, Plant Sci. 315 (2022) 111122.
[35] H. Ullah, R. Santiago-Arenas, Z. Ferdous, A. Attia, A. Datta, Chapter two - improving water use efficiency, nitrogen use efficiency, and radiation use efficiency in field crops under drought stress: a review, in: DL Sparks (Ed.), Adv. Agron, Academic Press, 2019, pp. 109–157.
[36] G.A. Carter, Primary and secondary effects of water content on the spectral reflectance of leaves, Am. J. Bot. 78 (1991) 916–924.
[37] B. Bayat, C. Van der Tol, W. Verhoef, Remote sensing of grass response to drought stress using spectroscopic techniques and canopy reflectance model inversion, Remote Sens 8 (2016) 557.
[38] A. Garg, S. Bordoloi, S.P. Ganesan, S. Sekharan, L. Sahoo, A relook into plant wilting: observational evidence based on unsaturated soil–plant-photosynthesis interaction, Sci. Rep. 10 (2020) 22064.
[39] F. Thenot, M. Méthy, T. Winkel, The Photochemical Reflectance Index (PRI) as a water-stress index, International Journal of Remote Sensing 23 (23) (2002) 5135–5139.
[40] C. Panigada, M. Rossini, M. Meroni, C. Cilia, L. Busetto, S. Amaducci, M. Boschetti, S. Cogliati, V. Picchi, F. Pinto, et al., Fluorescence, PRI and canopy temperature for water stress detection in cereal crops, Int. J. Appl. Earth Obs. Geoinformat. 30 (2014) 167–178.
[41] J.A. Gamon, J. Peñuelas, C.B. Field, A narrow-waveband spectral index that tracks diurnal changes in photosynthetic efficiency, Remote Sens. Environ. 41 (1992) 35–44.
[42] C. Van Der Tol, W. Verhoef, J. Timmermans, A. Verhoef, Z. Su, An integrated model of soil-canopy spectral radiances, photosynthesis, fluorescence, temperature and energy balance, Biogeosciences. 6 (2009) 3109–3129.
[43] S. Xu, J. Atherton, A. Riikonen, C. Zhang, J. Oivukkamäki, A. MacArthur, E. Honkavaara, T. Hakala, N. Koivumäki, Z. Liu, et al., Structural and photosynthetic dynamics mediate the response of SIF to water stress in a potato crop, Remote Sens. Environ. 263 (2021) 112555.
[44] K. Guan, J.A. Berry, Y. Zhang, J. Joiner, L. Guanter, G. Badgley, D.B. Lobell, Improving the monitoring of crop productivity using spaceborne solar-induced fluorescence, Glob Change Biol 22 (2016) 716–726.
[45] P. Muller, X.P. Li, K.K. Niyogi, Non-photochemical quenching. A response to excess light energy, Plant Physiol. 125 (2001) 1558–1566.
[46] Y. Peng, A.A. Gitelson, G. Keydan, D.C. Rundquist, W. Moses, Remote estimation of gross primary production in maize and support for a new paradigm based on total crop chlorophyll content, Remote Sens. Environ. 115 (2011) 978–989.
[47] C. Wu, Z. Niu, Q. Tang, W. Huang, B. Rivard, J. Feng, Remote estimation of gross primary production in wheat using chlorophyll-related vegetation indices, Agric. For. Meteorol. 149 (2009) 1015–1021.
[48] L.D. Prior, D. Eamus, G.A. Duff, Seasonal and diurnal patterns of carbon assimilation, stomatal conductance and leaf water potential in eucalyptus tetrodonta saplings in a wet–dry savanna in northern Australia, Aust. J. Bot. 45 (2) (1997) 241–258.
[49] M. Tester, P. Langridge, Breeding technologies to increase crop production in a changing world, Science 327 (5967) (2010) 818–822.